AWAD 2013

2013 Asia-Pacific Workshop on Fundamentals and Applications of Advanced Semiconductor Devices

June 26-28, 2013
Korea University, Seoul, Korea

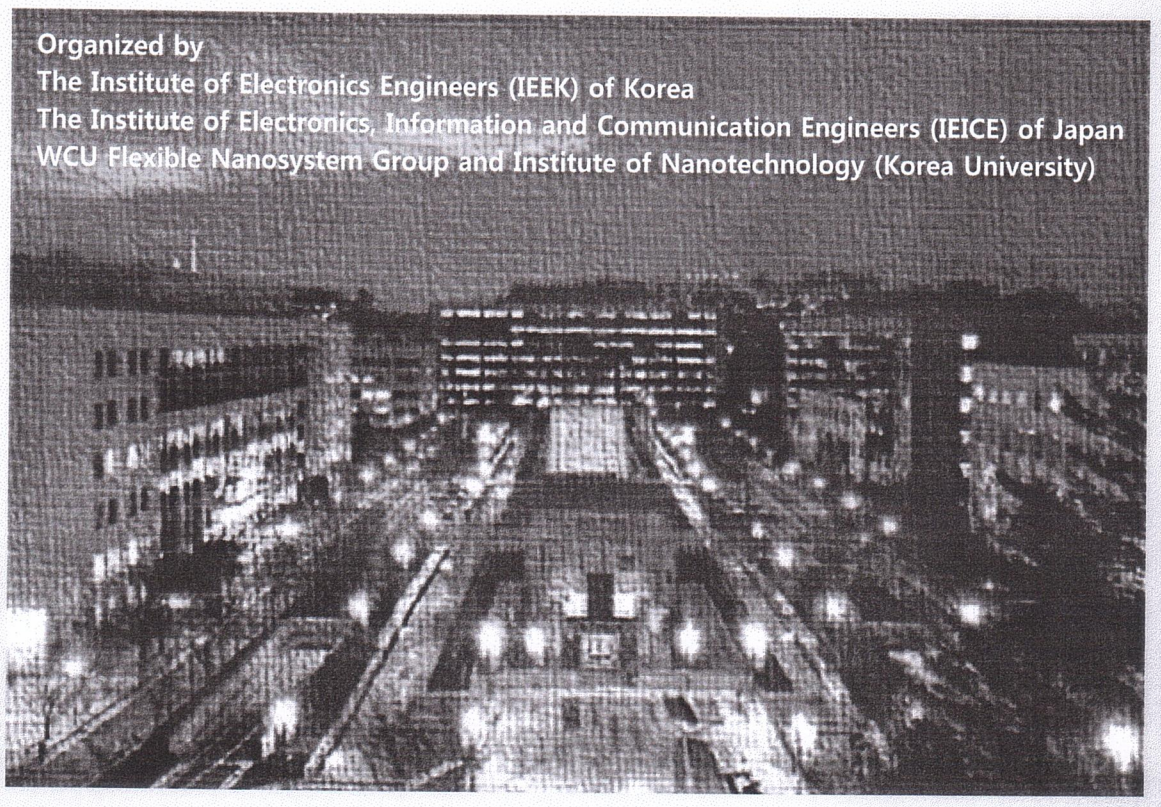

Sponsored by
National Center for Nanomaterials Technology (NCNT) , POSTECH
Samsung Advanced Institute of Technology (SAIT)
Electronics & Telecommunications Research Institute (ETRI)

Session 2B: Reliability and Characterization I

Session Co-Chairs: Woo Young Choi (Sogang Univ.), Rihito Kuroda (Tohoku Univ.)

2B-1 13:30 – 14:00

Invited talk : Density-of-States Based Modeling of Oxide Thin-Film Transistors: Toward Instability-Aware Design

Dae hwan Kim (Kookmin University)

2B-2 14:00 – 14:15

Proton irradiation effects on p- and n-type GaN

H. Okada, Y. Okada, H. Sekiguchi, A. Wakahara (Toyohashi University), S. Sato and T. Ohshima (Japan Atomic Energy Agency)

2B-3 14:15 – 14:30

Impact of Injected Carrier Types to Stress Induced Leakage Current Using Substrate Hot Carrier Injection Stress

H. W. Park, A. Teramoto, T. Inatsuka, R. Kuroda, S. Sugawa and T. Ohmi (Tohoku University)

Poster Session 14:45 – 15:30

Session Chair: Woo Young Choi (Sogang Univ.)

P-1 GaN epitaxy layer grown on Si (111) substrate using Ge buffer layer for extended CMOS integration

Yeon-Ho Kil, Young-Jae Park, Taek Sung Kim, Chang-Hee Hong, Chel-Jong Choi, and Kyu-Hwan Shim (Chonbuk National University)

P-2 Delay time component of InGaAs MOSFET caused by dynamic source resistance

Masayuki Yamada, Yasuyuki Miyamoto (Tokyo Tech.), and Ken Uchida (Keio Univ.)

P-3 Optimization of Mo-based, Au-free Ohmic contact for AlGaN/GaN-on-Si Heterostructure Field Effect Transistors

Shinhyuk Choi, Jae-Gil Lee, Hyungtak Kim and Ho-Young Cha (Hongik Univeristy)

P-4 Electrical Properties of Au/n-Ge Schottky Barrier Diode With Graphene Interlayer

Zagarzusem Khurelbaatar, Chel-Jong Choi, Gil-Song Kim, Daoheung Bouangeune, Keun-Soo Kim, Jung Tae Nam, Sang-Kwon Lee, Kyu-Hwan Shim (Chonbuk National University)

P-5 Electrostatic Discharge Natures for Transient Voltage Suppression Diodes Made of n+p-p+ and p+n-n+ Junctions

Daoheung Bouangeune, Zagarzusem Khurelbaatar, Sang-Sig Choi, Chel-Jong Choi, Deok-Ho Cho, and Kyu-Hwan Shim (Chonbuk National University)

P-6 Bidirectional Transient Voltage Suppression Diodes for the Protection of High Speed Data

2B-1

Density-of-States Based Modeling of Oxide Thin-Film Transistors: Toward Instability-Aware Design

Dae Hwan Kim,†‡ Kyung Min Lee†, Sung-Jin Choi†, and Dong Myong Kim†

†School of Electrical Engineering, Kookmin University, 861-1 Jeongneung-dong, Seongbuk-gu, Seoul 136-702, Korea
E-mail: ‡drlife@kookmin.ac.kr

Abstract The negative bias illumination stress (NBIS) has emerged as a serious hurdle to the successful industrialization and mass production of amorphous oxide thin-film transistor (TFT) technology. In this work, the subgap density-of-states (DOS) of amorphous In-Ga-Zn-O (a-IGZO) TFTs was extracted by combining the optical *C-V* and the generation-recombination current spectroscopy with the *I-V* model, named as DeAOTS (Density-of-states based Amorphous Oxide semiconductor Thin-film transistor Simulator). We also incorporated the recently proposed peroxide formation theory into our DOS model and simulation platform. Finally it was found that our DOS-based instability model reproduced the measured NBIS time-evolution of *I-V* characteristics of a-IGZO TFTs very well. Our results have the potential of playing a powerful role in the instability-aware design of oxide TFTs without a long-term stress and/or reliability test.

Keyword oxide thin-film transistor, density-of-states, instability model, peroxide, negative bias illumination stress.

1. Introduction

Amorphous oxide thin-film transistor (TFT) has been recognized as one of promising candidates substituting the amorphous silicon (a-Si), low temperature polycrystalline silicon (LTPS) and organic TFTs as switching/driving devices in the active-matrix liquid crystal displays (AMLCDs) and/or the active-matrix organic light emitting diode displays (AMOLEDs), because of its advantages of the flexibility, visible light transparency, large-area uniformity of a low temperature sputter-deposited amorphous material, and quite high carrier mobility (Table 1). In real, very recently, various display backplanes driven by oxide TFTs have been competitively demonstrated [1]-[3]. Especially, the compatibility of bottom gate-structured oxide TFTs with the a-Si TFT-based TFT-LCD manufacturing line makes them promising solutions as the cost-effective driving devices for AMOLEDs in comparison with top gate-structured LTPS TFTs. However, the photoelectric stress-induced instabilities have emerged as challenging issues for industrialization of the oxide TFT-driven display backplanes [4], [5]. Therefore, the fundamental understanding and quantitative projection of instability became more important and indispensable for the systematic design of the oxide TFT materials, devices, and circuits. In specific, the negative bias illumination stress (NBIS)-induced instability needs to be intensively analyzed because in either AMLCDs or AMOLED display backplane, switching TFTs are commonly subject to the negative gate-to-source voltage (V_{GS}) and positive drain-to-source voltage (V_{DS}) stress under photo-illumination during most of each frame time [4].

Table 1 Comparison of TFT active materials

TFT active material	a-Si	LTPS	Oxide
Field effect mobility	~1 cm^2/Vs	~100 cm^2/Vs	>10 cm^2/Vs
TFT uniformity	good	poor	good
Transparency	poor	poor	good
Process temperature	~250C°	>250C°	>RT
Fabrication technique	PECVD	PECVD	sputtering
Channel type	NMOS	PMOS (CMOS)	NMOS
Cost	low	high	low
Yield	-	medium	medium

In this work, we quantitatively investigated the NBIS-induced threshold voltage shift (ΔV_T) in amorphous In-Ga-Zn-O (a-IGZO) TFTs and established its physical model and simulation platform based on experimentally extracted density-of-states (DOS). In order to extract subgap DOS of TFT active material and calculate the TFT *I-V* characteristics, the *optical C-V spectroscopy* [6], the *generation-recombination current* (I_{G-R}) *spectroscopy* [7], and the improved *DeAOTS* (Density-of-states based Amorphous Oxide semiconductor Thin-film transistor Simulator) [8], [9] were conjointly used. Finally, it was

found that our peroxide formation [10]-based instability model successfully reproduced the NBIS time (t_{NBIS})-evolution of the measured *I-V* characteristics.

2. DOS Extraction

The subgap DOS in oxide semiconductor thin-film which acts as the active material of oxide TFTs can be schematically illustrated as shown in Fig. 1. Among DOS parameters, the $g_A(E)$ [$cm^{-3}eV^{-1}$], *i.e.*, the acceptor-like states near the conduction band minimum (CBM: E_C), which are known to originate from the disorder of metal cation *s*-bands, namely, In-O-metal bonding angle variation in the case of a-IGZO and denote the degree of strong dispersion of electronic structures near E_C [11]-[13], determine the *I-V* characteristics including the subthreshold swing (SS). On the other hand, the $g_{TD}(E)$ [$cm^{-3}eV^{-1}$], *i.e.*, the donor-like states near the valence band maximum (VBM: E_V), originate either from the amorphous randomness, namely, the oxygen *p*-band disorder (intrinsic) or from the deep level donors (extrinsic). While the former reflects the degree of strongly localized states near E_V, namely, a weak dispersion of holes, the latter can be identified by oxygen vacancy (V_O) defects with the inward relaxation with neighboring metal atoms followed by the large vacancy size [14]. The $g_{TD}(E)$ is closely related to the photoelectric stress-induced instability [4] and the N_{SD} [cm^{-3}] works as the density of shallow donors, *i.e.*, *n*-type doping concentration, for supplying free carriers. In addition, the V_Os of oxide films indirectly but strongly affects the concentration of shallow donors (N_{SD}) by transforming them to shallow donors through their interaction either with metal cations [15] or with hydrogen species [16], although they are energetically favored to be deep donors [17], [18].

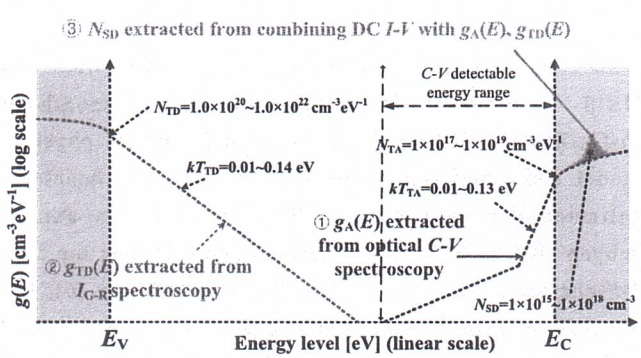

Fig. 1 The schematic illustration of subgap DOS with its extraction technique.

The used a-IGZO TFTs had the etch stopper-type and were integrated with circuits integrated on a glass substrate as shown in Fig. 2. The bottom-gate and top contact structured TFTs were fabricated using the standard semiconductor processes. The detailed process was given in [9].

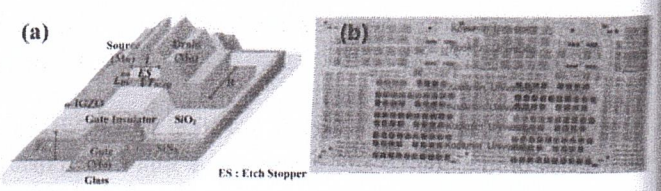

Fig. 2 (a) A schematic illustration of integrated a-IGZO TFT. (b) The photograph of a-IGZO TFTs and circuits integrated on a glass substrate [9].

The fabricated a-IGZO TFT has a gate dielectric thickness T_{OX}=258 nm as an equivalent oxide thickness (EOT) (400/50 nm of SiN_X/SiO_X bilayer), the channel width W=200 μm, the channel length L=100 μm, the gate-to-S/D overlap length Lov=10 μm, and the thickness of a-IGZO thin-film T_{IGZO}=50 nm. Typical device parameters were obtained to be the ON current I_{DS}=1.13 [μA] at V_{GS}=V_{DS}=10.1 [V], V_{ON}=2.8 [V] (V_{ON} was defined as V_{GS} at I_{DS}=1 [pA] in the transfer curve), the threshold voltage V_T=7.2 [V] (defined as V_{GS} at I_{DS}=10 [nA] in the transfer curve), the SS=0.74 [V/dec], the field-effect mobility (μ_{FE})=9.4 [cm^2/Vs] at V_{GS}=20 [V] and V_{DS}=0.1 [V], and the I_{ON}/I_{OFF} ratio=5.35×10⁶.

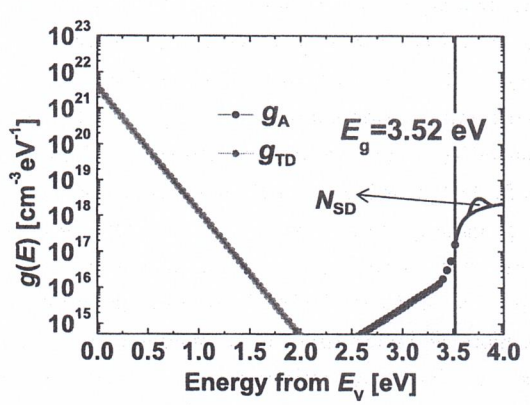

Fig. 3 The extracted subgap DOS of a-IGZO TFT.

The extracted subgap DOS of a-IGZO TFTs was shown in Fig. 3. First of all, the $g_A(E)$ was extracted by using the optical *C-V* spectroscopy [6]. It was found that the $g_A(E)$ was fitted very well with the superposition of two exponential formulae as follows:

$$g_A(E) = N_{DA} \times \exp\left(\frac{E-E_C}{kT_{DA}}\right) + N_{TA} \times \exp\left(\frac{E-E_C}{kT_{TA}}\right) \quad (1)$$

where the extracted parameters were N_{TA}=2.54×10^{17} [cm^{-3}eV^{-1}], kT_{TA}=0.01 [eV], N_{DA}=2.84×10^{16} [cm^{-3}eV^{-1}], and kT_{DA}=0.23 [eV]. The value of N_{TA} was relatively lower than that of a-Si TFTs (N_{TA}=10^{21} [cm^{-3}eV^{-1}] for a-Si [19]). Subsequently, the extraction of $g_{TD}(E)$ was done by the I_{G-R} spectroscopy [7]. When the $g_{TD}(E)$ was assumed to be one exponential function, it could be modeled as

$$g_{TD}(E) = N_{TD} \times \exp\left(\frac{E_V-E}{kT_{TD}}\right) \quad (2)$$

where the extracted parameters were N_{TD}=4.0×10^{21} [cm^{-3}eV^{-1}] and kT_{TD}=0.125 [eV]. Finally, a technique of combining the optical C-V spectroscopy [6] and the I_{G-R} spectroscopy [7] with the improved DeAOTS [8], [9] was used for the extraction of N_{SD}. The extracted value was N_{SD}=1.77×10^{16} [cm^{-3}].

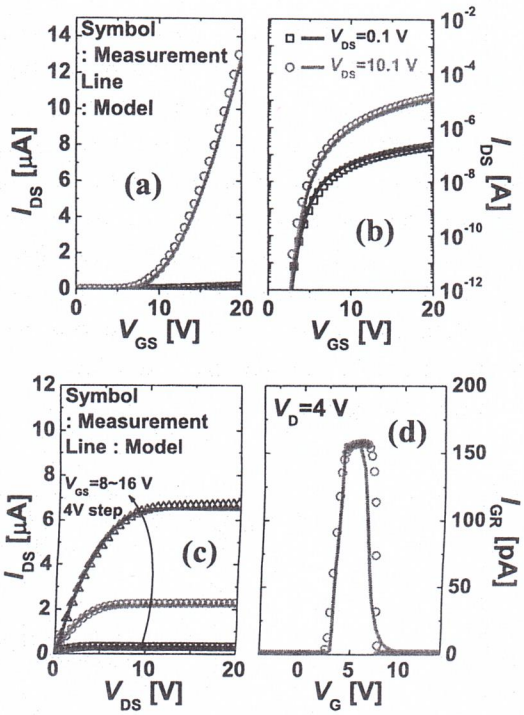

Fig. 4 The measured I-V characteristics of a-IGZO TFTs (symbols) in comparison with the calculated ones by DeAOTS (lines). (a) The transfer curve in a linear scale, (b) the transfer curve in a log scale, (c) the output curve, and (d) the I_{G-R} curve.

Based on the extracted DOS parameters, both the $I_{DS}(V_{GS}, V_{DS})$ and the $I_{G-R}(V_G, V_D)$ characteristics were calculated by using DeAOTS [8], [9]. As shown in Fig. 4, the calculated $I_{DS}(V_{GS}, V_{DS})$ and $I_{G-R}(V_G, V_D)$ curves agreed very well with the measured ones. Our results verify that all of the extracted parameters, the implemented $I_{DS}(V_{GS}, V_{DS})$ and $I_{G-R}(V_G, V_D)$ models, and the parameter-extracting methodology can successfully reproduce the measured electrical characteristics even for the subthreshold region as well as for $V_{GS}>V_T$. Furthermore, the proposed method can be a main step triggering the process optimization, device characterization, and modeling for a systematic design and implementation of oxide TFT circuits and applications because DOS is the process-controlled parameter.

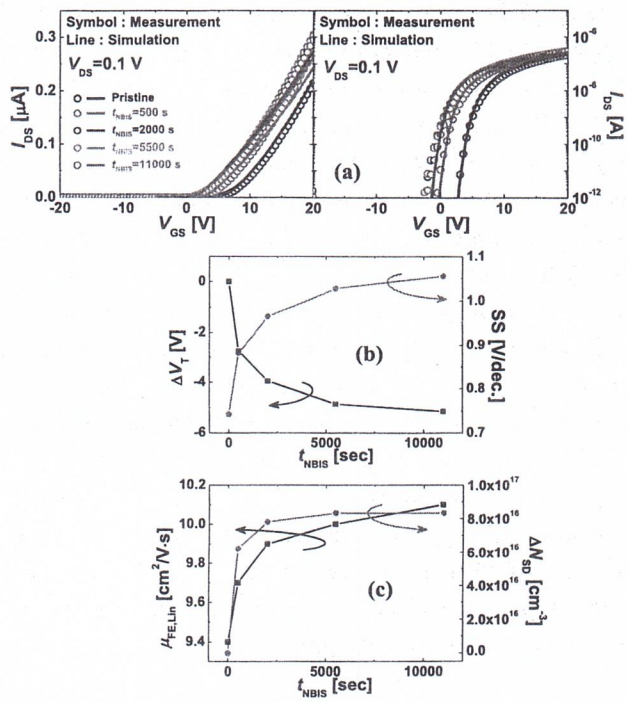

Fig. 5 (a) The measured t_{NBIS}-evolution of transfer characteristics (symbols) in comparison with the model (lines). (b) The measured t_{NBIS}-evolutions of ΔV_T and SS. (c) The t_{NBIS}-evolutions of the measured μ_{FE} (in linear operation regime) and the model-based ΔN_{SD}.

3. DOS-Based Instability Models

In order to establish the DOS-based instability model, the IGZO TFT I-V characteristics were measured with the increase of t_{NBIS}. The conditions of NBIS were V_{GS}=-20 V, V_{DS}=10 V, and t_{NBIS} from 0 to 11000 sec, which are consistent with AMLCD switching TFTs during the most of each frame time. The illumination was applied by a commercial LED backlight unit with a brightness of 300

[cd/m^2]. During the NBIS test, all the electrical properties were measured with halting the NBIS, by using Agilent 4156 semiconductor parameter analyzer under dark and ambient backlight illumination condition at room temperature. As shown in symbols of Fig. 5(a), the NBIS-induced ΔV_T without a significant change of SS is observed to be –2.75/–3.95/–4.86/–5.15 [V] after NBIS for 500/2000/5500/11000 sec, respectively. The measured t_{NBIS}-evolutions of ΔV_T, SS, and μ_{FE} (in linear operation regime) were also summarized in Fig. 5(b) and (c).

Regarding this widely observed NBIS-induced negative ΔV_T of IGZO TFTs, the valence band tail (VBT) hole (h^+)-intermediated formation of the O Frenkel-pair defect, in other words, peroxide state (O_2^{2-}), was very recently suggested as a microscopic origin for the NBS/NBIS-induced instability [10]. Because the VBT states of IGZO films have a $pp\sigma^*$ anti-bonding character, the anti-bonding state is empty by excited holes in $g_{TD}(E)$ under NBIS, and the photo-illumination makes the two oxygen atoms prefer to bond as O_2^{2-}. While the mechanism from the pristine to peroxide state via the transition state (see the inset of Fig. 6) can be denoted by $O^{2-}+O^{2-}+2h^+ \rightarrow O_2^{2-}$ as well as $O^{2-}+O^{2-}+2e^-+2h^+ \rightarrow O_2^{2-}+2e^-$ (electron doping), the recovery mechanism can be described as $O_2^{2-}+2e^- \rightarrow O^{2-}+O^{2-}$ (from the peroxide to pristine state). Here, this peroxide state is the meta-stable state and is recovered very slowly after eliminating NBIS, which is due to the relatively higher energy barrier (β in [10]). By the process of $O^{2-}+O^{2-}+2e^-+2h^+ \rightarrow O_2^{2-}+2e^-$ (electron doping), the formation of O_2^{2-} acts as the increase of (2+) donors and is followed by the parallel shift of IGZO TFT I_{DS}-V_{GS} curves into the negative V_{GS} direction [as seen in Fig. 5(a)].

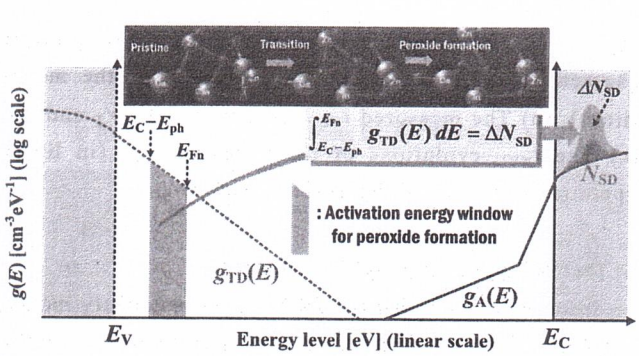

Fig. 6 The schematic diagram illustrating the increase of N_{SD} (ΔN_{SD}) resulting from the VBT hole-intermediated peroxide formation, which can be quantified by the activation energy window for peroxide formation in $g_{TD}(E)$ under NBIS. The inset shows the atomic structures from the pristine to peroxide configurations via the transition calculated in a-IGZO. The equation in the yellow box suggests that the area of the activation energy window for peroxide formation is exactly the same as ΔN_{SD}.

Thus, we incorporated this microscopic view into the device simulation platform for instability-aware design. For a more quantitative model, we defined the area of $\int_{E_C-E_{ph}}^{E_{Fn}} g_{TD}(E)dE$ as the "activation energy window for peroxide formation" (Fig. 6), where E_{Fn}= the quasi-Fermi energy level and E_{ph}=the photon energy. According to the peroxide model, the IGZO TFT with a smaller activation energy window would be definitely more stable under NBIS and the increase of N_{SD} (ΔN_{SD}) resulting from the O_2^{2-} formation can be calculated by using the relation of $\Delta N_{SD}= \int_{E_C-E_{ph}}^{E_{Fn}} g_{TD}(E)dE$ (Fig. 6) with all parameters-incorporating DeAOTS. Based on our model, we tried to trace the t_{NBIS}-evolution of I-V characteristics by updating the stress time-varying DOS in the next stress time spot from one in the former time spot and repeating these update procedures time step by step (Fig. 7). With using $E_{ph,eff}$=2.49 eV as empirical parameter, surprisingly, we found that the measured t_{NBIS}-evolution of I_{DS}(V_{GS}, V_{DS}) could be reproduced as seen in the lines of Fig. 5(a). The t_{NBIS}-evolution of the calculated N_{SD} was also shown in Fig. 5(c). With the increase of t_{NBIS}, the moving up of E_{Fn} (at NBIS condition) toward E_C becomes retarded, which supports the quantitative simulation of the saturated ΔV_T during NBIS.

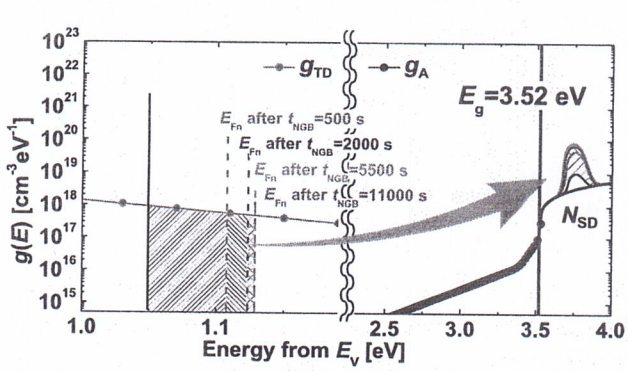

Fig. 7 The t_{NBIS}-evolution of the E_{Fn} with $E_{ph,eff}$=2.49 eV and the activation energy window for peroxide formation.

This suggests that the t_{NBIS}-induced ΔV_T can be described with the exact function of not only the material

and process-controlled parameters, e.g., DOS, the device geometric parameters, e.g., T_{IGZO} and T_{OX}, but also the stress condition, e.g., gate bias, E_{Fn} at bias stress, and E_{ph}. For instance, the oxide TFT-A which has a relatively smaller area of the activation energy window shows the smaller stress-induced ΔV_T under specific stress conditions than that shown in the other oxide TFT-B which has relatively larger area of the activation energy window compared with that of TFT-A. The t_{NBIS}-evolution of either all electrical characteristics or the subgap DOS of a-IGZO TFTs can be also calculated precisely by using our methodology and parameter set.

4. Conclusions

We showed that the t_{NBIS}-evolution of the electrical characteristics of a-IGZO TFTs could be calculated and projected through our model based on the activation energy window of the VBT hole-intermediated peroxide formation. Therefore, our results have the potential of playing a powerful role in the instability-aware design of oxide TFTs without a long-term stress test, and also are consistent with the recently formulated O Frenkel-pair defect theory.

Acknowledgements

This work was supported by the National Research Foundation of Korea (NRF) grant funded by the Ministry of Education, Science and Technology (MEST) (Grant no. 2012-0000147).

References

[1] Y. Ohta et al.: Amorphous In-Ga-Zn-O TFT-LCDs with high reliability, in Proc. Int. Display Workshop, Dec. 2009, 1685–1688.

[2] J. Sakata et al.: Development of 4.0-in. AMOLED display with driver circuit using amorphous In-Ga-Zn-Oxide TFTs, in Proc. Int. Display Workshop, Dec. 2009, 689–692.

[3] J.-H. Lee et al.: World's largest (15-inch) XGA AMLCD panel using IGZO oxide TFT, in Proc. SID Int. Symp., May 2008, 625–628.

[4] Y. Kim et al.: Amorphous InGaZnO thin-film transistors–Part II: Modeling and simulation of negative bias illumination stress-induced instability, IEEE Tran. Electron Devices 59, 2699–2706 (2012).

[5] T. Kamiya et al.: Present status of amorphous In-Ga-Zn-O thin-film transistors, Sci. Technol. Adv. Mater. 11, 044305 (2010).

[6] J.-H. Park et al.: Extraction of Density of States in Amorphous GaInZnO Thin Film Transistors by Combining an Optical Charge Pumping and Capacitance-Voltage Characteristics, IEEE Electron Device Lett. 29, 1292–1295 (2008).

[7] M. Bae et al.: Extraction of Subgap Donor States in a-IGZO TFTs by Generation-Recombination Current Spectroscopy, IEEE Electron Device Lett. 32, 1248–1250 (2011).

[8] Y. W. Jeon et al.: Subgap Density-of-States Based-Amorphous Oxide Thin Film Transistor Simulator (DeAOTS), IEEE Trans. Electron Devices 57, 2988–3000 (2010).

[9] Y. Kim et al.: Amorphous InGaZnO thin-film transistors–Part I: Complete extraction of density of states over the full subband-gap energy range, IEEE Tran. Electron Devices 59, 2689–2698 (2012).

[10] H.-H. Nahm et al.: Instability of amorphous oxide semiconductors via carrier-mediated structural transition between disorder and peroxide state, Phys. Status Solidi B 249, 1277–1281 (2012).

[11] J. Robertson: Physics of amorphous conducting oxides. J. Non-Cryst. Solids 354, 2791 2795 (2008).

[12] T. Kamiya et al.: Electronic structure of oxygen deficient amorphous oxide semiconductor a-InGaZnO4–x: Optical analyses and first-principle calculations, Phys. Status Solidi C 5, 3098–3100 (2008).

[13] T. Kamiya et al.: Electronic structure of the amorphous oxide semiconductor a-InGaZnO4-x: Tauc-Lorentz optical model and origins of subgap states, Phys. Status Solidi A 206, 860–867 (2009).

[14] T. Kamiya et al.: Origins of high mobility and low operation voltage of amorphous oxide TFTs: Electronic structure, electron transport, defects and doping, J. Display Tech. 5, 273–288 (2009).

[15] Y.-S. Kim and C. H. Park: Rich variety of defects in ZnO via an attractive interaction between O vacancies and Zn interstitials: origin of n-type doping, Phys. Rev. Lett. 102, 086403 (2009).

[16] A. Janotti and C. G. Van deWalle: Hydrogen multicenter bonds, Nature Mater. 6, 44–47 (2007).

[17] A. Janotti and C. G. Van deWalle: Native point defects in ZnO, Phys. Rev. B 76, 165202 (2007).

[18] J. Robertson: Disorder and instability processes in amorphous conducting oxides, Phys. Status Solidi B 245, 1026–1032 (2008).

[19] J. Kanicki and S. Martin, in *Thin-Film Transistors*, edited by C. R. Kagan and P. Andry (Dekker, New York, 2003), 71–137.